Soft Matter

PAPER

Cite this: *Soft Matter*, 2017, **13**, 1554

Synthesis of polyacid nanogels: pH-responsive sub-100 nm particles for functionalisation and fluorescent hydrogel assembly†

Amir H. Milani,*[a] Jennifer M. Saunders,[a] Nam T. Nguyen,[a] Liam P. D. Ratcliffe,[b] Daman J. Adlam,[c] Anthony J. Freemont,[c] Judith A. Hoyland,[cd] Steven P. Armes[b] and Brian R. Saunders*[a]

Received 5th December 2016,
Accepted 19th January 2017

DOI: 10.1039/c6sm02713j

rsc.li/soft-matter-journal

Nanogels are crosslinked polymer particles with a swollen size between 1 and 100 nm. They are of major interest for advanced surface coatings, drug delivery, diagnostics and biomaterials. Synthesising polyacid nanogels that show triggered swelling using a scalable approach is a key objective of polymer colloid chemistry. Inspired by the ability of polar surfaces to enhance nanoparticle stabilisation, we report the first examples of pH-responsive polyacid nanogels containing high –COOH contents prepared by a simple, scalable, aqueous method. To demonstrate their functionalisation potential, glycidyl methacrylate was reacted with the –COOH chemical handles and the nanogels were converted to macro-crosslinkers. The concentrated (functionalised) nanogel dispersions retained their pH-responsiveness, were shear-thinning and formed physical gels at pH 7.4. The nanogels were covalently interlinked *via* free-radical coupling at 37 °C to form transparent, ductile, hydrogels. Mixing of the functionalised nanogels with polymer dots enabled covalent assembly of fluorescent hydrogels.

Introduction

Crosslinked polymer particles containing –COOH groups that are swollen at physiological pH are important for advanced surface coatings,[1] biomaterials research,[2] rheological additives[3] and cosmetics.[4] These particles are termed microgels when the size is between 10^2 and 10^5 nm[5] and have been studied as blood-cell mimics,[6] cell-laden particles,[7] emulsion stabilisers,[8,9] light responsive systems[10,11] and for tissue regeneration.[12] Nanogels are crosslinked polymer particles with a swollen size of 1 to 100 nm.[5,13] Unfortunately, this nanogel definition has not been universally adopted and many microgels have been (incorrectly) termed nanogels. Nanogels are highly desirable because of their high surface areas for functionalisation,[14] fast response times to an external stimulus,[15] enhanced circulation times *in vivo*[16] and optical transparency.[15] This combination of properties has led to their use as imaging agents,[17] surface coatings,[18] pastes,[19] diagnostic systems[20] and delivery.[15,20] Polyacid nanogels which contain a high concentration of –COOH groups are potentially widely useful, especially if they show pH-triggered swelling at physiological pH. The latter behaviour should favour *in vivo* release and such functionality is well-suited to derivatisation reactions.[21] Although a number of studies have reported pH-responsive nanogels,[13–15] publications that report measured swollen diameters between 1 and 100 nm (*i.e.*, genuine nanogels) are rare[13] and examples of polyacid nanogels are absent. Polyacid nanogels are a missing class of gel particles. Whilst several methods to prepare polyacid microgels have been established[22,23] a scalable synthesis for genuine polyacid nanogels is urgently needed. These methods have included emulsion polymerisation with[22] or without[23,24] subsequent hydrolysis. Here, a new nanogel platform technology is established and the particles are functionalised to give novel, injectable and fluorescent gels.

Recently, a semicontinuous emulsion polymerisation strategy for preparing sub-100 nm polymer nanoparticles (termed nanolatexes) was pioneered.[25] The study demonstrated that copolymerising a small proportion of methacrylic acid (MAA) with methyl methacrylate (MMA) increased the surface area which could be stabilised by the surfactant molecules.[25] Accordingly, we hypothesised that by greatly increasing the MAA content,

[a] *School of Materials, University of Manchester, Manchester, M13 9PL, UK. E-mail: amirhossein.milani@manchester.ac.uk*
[b] *Department of Chemistry, The University of Sheffield, Dainton Building, Brook Hill, Sheffield, South Yorkshire, S3 7HF, UK*
[c] *Division of Cell Matrix Biology and Regenerative Medicine, Faculty of Biology, Medicine and Health, University of Manchester, Oxford Road, Manchester, M13 9PL, UK*
[d] *NIHR Manchester Musculoskeletal Biomedical Research Unit, Manchester Academic Health Science Centre, Manchester, UK*

† Electronic supplementary information (ESI) available: Potentiometric titration data, SEM images, rheology data, swelling measurements, biocompatibility data, UV-Vis, TEM images and PL spectra. See DOI: 10.1039/c6sm02713j

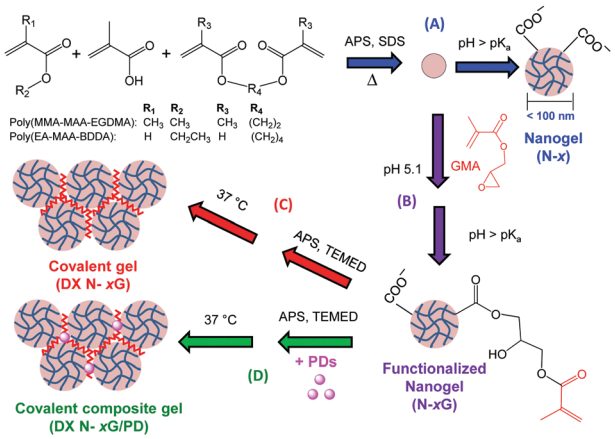

Scheme 1 Schematic for synthesis of pH-responsive nanogels (N-*x*), functionalised nanogels (N-*x*G) and doubly crosslinked nanogels (DX N-*x*G). Polymer dots (PDs) were mixed with N-1G and N-1G interlinked to give DX N-1G/PD composite hydrogels. APS, SDS and TEMED are ammonium persulfate, sodium dodecylsulfate and *N*,*N*,*N*′,*N*′-tetramethylethylenediamine.

and including a crosslinking monomer, semicontinuous emulsion polymerisation could enable synthesis of genuine polyacid nanogels using a scalable protocol. The high –COOH concentrations within the nanogels introduced in this work enabled functionalisation whilst retaining strong pH-triggered swelling.

In this study four nanogel systems were synthesised (N-*x*, *x* = 1–4) (see Scheme 1A) using semicontinuous, starved-feed, emulsion polymerisation. A comonomer solution was fed into a sodium dodecyl sulfate (SDS) solution containing initiator (ammonium persulfate, APS) at 80 °C. The nanogels comprised poly(methyl methacrylate-*co*-MAA-*co*-ethylene glycol dimethacrylate) (poly(MMA–MAA–EGDMA)) or poly(ethylacrylate-*co*-MAA-*co*-1,4-butanediol diacrylate) (poly(EA–MAA–BDDA)). Vinyl-functionalised nanogels (N-*x*G) were prepared (Scheme 1B) from the nanogels using glycidyl methacrylate (GMA). Concentrated N-*x*G dispersions became viscous when the pH was increased and inter-nanogel covalent linking occurred in the presence of APS to give doubly crosslinked nanogels (DX N-*x*G) (Scheme 1C). As a proof-of-concept study, mixed N-*x*G dispersions/polymer dot (PD) dispersions were prepared and cured to obtain DX N-*x*G/PD composite gels as depicted in Scheme 1D.

In a previous study it was shown that concentrated dispersions of polyacid microgels functionalised with vinyl groups could be converted to pH-responsive macroscopic hydrogels *via* double crosslinking.[23] Those hydrogels, which were termed doubly crosslinked microgels (DX MGs), could support biomechanically meaningful loads.[26] However, the unconfined gels were relatively brittle compared to high performance gels[27] and were also turbid. Here, we show that functionalised polyacid nanogels enable assembly of transparent doubly crosslinked nanogels (DX NGs) with improved ductility. Taking advantage of the high transparency of the nanogels, we also prepared a new class of fluorescent composite hydrogels containing polymer dots.

Experimental section

Materials

Methacrylic acid (MAA, 99%), methyl methacrylate (MMA, 98.5%), ethylene glycol dimethacrylate (EGDMA, 98%), ethyl acrylate (EA, 99%), 1,4-butanediol diacrylate (BDDA, 90%), glycidyl methacrylate, (GMA, 97%), ammonium persulfate (APS, 98%), sodium dodecyl sulphate (SDS, 98.5%), *N*,*N*,*N*′,*N*′-tetramethylethylenediamine (TEMED, 99%). 2,5-Bis(octyloxy)terephthalaldehyde (98%), terephthalaldehyde (99%), 1,4-phenylenediacetonitrile (98%), tetrabutylammonium hydroxide (TBAH, 1.0 M in methanol), chloroform (>99%) and Tween 80 were all purchased from Aldrich. All monomers were used as received. Ultra-high purity deionised water was used for all experiments.

Synthesis of vinyl-functionalised nanogels

Four nanogels (N-*x*, *x* = 1 to 4) were synthesised *via* semicontinuous emulsion polymerisation with different monomer compositions as shown in Table 1. N-1, N-2 and N-3 nanogels comprised poly(MMA–MAA–EGDMA) whilst N-4 comprised poly(EA–MAA–BDDA). N-1 and N-4 contained the highest crosslinker concentrations (1.0 mol%) and enabled the effect of primary monomer type to be studied. N-2 and N-3 were synthesised using lower crosslinker contents (0.5 mol%). The synthesis for N-1 is given as an example. Briefly, SDS (1.2 g, 4.0 mmol) was dissolved in water (240 mL) and the solution purged with nitrogen for 30 min. Then APS (0.20 g, 0.90 mmol) in water (2.0 mL) was added. The semicontinuous emulsion polymerisation was conducted at 80 °C. A co-monomer solution containing MMA (42.0 g, 0.42 mol), MAA (10.0 g, 0.12 mol) and EGDMA (1.1 g, 5 mmol) was added at a feed rate of 0.30 mL min^{-1}. The reaction was left to stir for 1 h after the feed finished and then the reaction cooled to room temperature. The dispersion was dialysed against water for 10 days. Nanogels N-2, N-3 and N-4 were prepared using the same general conditions and the quantities given in Table 1.

For GMA functionalisation, the pH of the nanogel dispersion (120 g, 5 wt%) was adjusted to 5.1 then GMA (4.5 g, 0.39 mol) was added while stirring. The dispersion was left to stir for 8 h

Table 1 Quantities of monomers used for nanogel synthesis

Code	MMA/g	EA/g	MAA/g	EGDMA/g	BDDA/g	MAA/mol%	Crosslinker/mol%	Particle conc'n[a]/wt%
N-1	42.0	—	10.00	1.10	—	24.0	1.0	12.0
N-2	35.2	—	9.05	0.439	—	29.8	0.5	15.7
N-3	44.9	—	7.39	0.528	—	20.9	0.5	18.0
N-4	—	10.7	2.55	—	0.271	24.4	1.0	5.3

[a] Based on mass of monomer used.

at 40 °C. The dispersion was washed with chloroform twice and residual solvent removed by rotary evaporation.

Synthesis of control microgel

The control microgel used for Fig. 1d was synthesised using seed-feed emulsion polymerisation and followed a method similar to that described previously.[23] For a typical preparation, SDS (1.6 g, 5.5 mmol) was first dissolved in water (517.0 g) and this solution was purged by nitrogen for 30 min while the temperature was kept at 80 °C. A comonomer mixture was prepared containing MMA (186.0 g, 1.86 mol), MAA (98.0 g, 1.14 mole) and EGDMA (1.0 g, 5.0 mmol). A portion of the comonomer mixture (16.0 g) was added to the water/SDS solution and left to stir for 5 min. Then, K_2HPO_4 (0.17 g, 0.98 mmol) and APS (0.07 g, 0.31 mmol) were added to the reaction vessel. After 30 min the remaining monomer and water (150 g) was added at a rate of 1 mL min^{-1}. The reaction was left to stir for 1 h after the feed was finished and then the reaction was quenched with ice.

Synthesis of conjugated polymer dots

The structures and codes used for the conjugated polymer dots (PDs) are shown in Fig. 3a. The codes used are based on the wavelength of maximum photoluminescence intensity (λ_{max}, see Fig. S9, ESI†). Thus, P605 and P670 PDs had λ_{em} values of 605 and 670 nm, respectively. Both PD types were prepared using a modified procedure that originally established by Kim *et al.*[28] *In situ* colloidal Knoevenagel polymerisation was conducted with equimolar dialdehyde and diacetonitrile monomers in an aqueous emulsion using Tween 80 as the surfactant. The molar ratio of [dialdehyde]:[diacetonitrile]:[Tween 80] was fixed at [1.00]:[1.00]:[11.57]. The typical protocol for the synthesis of P670 PD synthesis was as follows. The reagents 2,5-bis(octyloxy)terephthalaldehyde (23.2 mg, 0.059 mmol) and 1,4-phenylenediacetonitrile (9.27 mg, 0.059 mmol) were dissolved in Tween 80 (0.9 g) in a 25 mL round bottom flask at 65 °C. Water (15 mL) was then added at 65 °C over a period of 90 min at a constant rate of 0.17 mL min^{-1}. A clear dispersion was obtained which was then cooled to room temperature over a period of 30 min prior to addition of TBAH (0.6 mL). The polymerisation was conducted over 14 hours at room temperature with magnetic stirring. The product was purified by extensive dialysis.

Preparation of doubly crosslinked nanogels

To prepare DX N-1G with solid content of 12 wt%, GMA functionalised NG (*i.e.*, N-1G) (1.00 g, 14.7 wt%) was vortexed with APS solution (69 μL, 78 mM), water (50 μL) and alkaline TEMED solution (51 μL). The latter contained NaOH (4 M) with TEMED at a volume ratio of 48:2. Addition caused a viscosity increase and the pH also increased to 7.4. The viscous fluid was transferred into an o-ring (outer diameter = 15 mm and thickness = 1 mm) and sandwiched between two glass slides and cured at 37 °C overnight. The same procedure was used to prepare DX N-4G gels.

For preparation of DX NG/PD composite gels, N-1G (1.00 g, 14.7 wt%) was mixed with PD dispersion (0.50 g, 1 wt%). APS solution (69 μL, 78 mM) and alkaline TEMED solution (51 μL, described above) was then added and the dispersion cured at 37 °C overnight using the o-ring mould as described above.

Physical measurements

Potentiometric titration data were obtained in the presence of aqueous 0.05 M NaCl using a Mettler Toledo titrator. Dynamic light scattering (DLS) and zeta potential data were obtained using a Malvern Zetasizer NanoZS instrument. A Hitachi U-1800 spectrophotometer was used for UV-visible spectroscopy measurements. SEM images were obtained using Philips FEGSEM at 6 kV. For TEM first the copper TEM grids (Agar Scientific, UK) were surface-coated in-house to yield a thin film of amorphous carbon. The grids were then plasma glow-discharged for 40 s to create a hydrophilic surface. The particle dispersion (0.20% w/w, 11 μL) was placed onto a freshly glow discharged grid for 1 min and then blotted with filter paper to remove excess solution. To stain the deposited nanoparticles, a 0.75% w/w aqueous solution of uranyl formate (9 μL) was placed *via* micropipette on the sample-loaded grid for 20 s and then carefully blotted to remove excess stain. Each grid was then carefully dried using a vacuum hose. Imaging was performed at 100 kV using a Phillips CM100 instrument equipped with a Gatan 1k CCD camera. Number-average diameters were determined using Image-J (NIH) software. Dynamic rheology measurements used a TA Instruments AR G2 rheometer. A 20 mm diameter plate geometry was used and the gap was set to 2500 μm. The photoluminescence (PL) spectra were obtained using an Edinburgh Instruments FLS980 spectrometer.

The volume swelling ratio of DX 1-NG was measured using a gravimetric method. Samples were placed in phosphate buffer solution at different pH values (0.1 M). Each sample was weighed once a day and left in a fresh buffer. This process was repeated for 5 days. The volume–swelling ratio (Q_{DX}) for the DX NG was calculated using following equation:

$$Q_{DX} = \rho_p \left(\frac{Q_{(m)}}{\rho_s} + \frac{1}{\rho_p} \right) - \frac{\rho_p}{\rho_s}$$

where $Q_{(m)}$ is the mass swelling ratio. The parameters ρ_s and ρ_p are the densities of the solvent (water) and polymer, respectively. These values were taken as 1.0 and 1.2 g mL^{-1}.[29]

Cytotoxicity studies

Human nucleus pulposus (NP) cells, were cultured in Dulbecco's modified Eagle's medium supplemented with 10% fetal bovine serum (FBS, Gibco), L-ascorbic acid 2-phosphate (10 μM) and antibiotic/antimycotic (Sigma-Aldrich, UK) at 37 °C in a humidified 5% CO_2 atmosphere. Cells were seeded at a density of 5×10^4 per well onto 24-well plates and cultured for 24 h. Gel samples (20 mg), sterilised with 70% ethanol and washed with phosphate buffered saline (PBS) were introduced using 0.4 μm cell-culture inserts (BD Biosciences, UK). MTT assays (Aldrich, UK) were performed after 1, 2 and 3 days and the results compared against an empty insert control. There were three points per

time-point (n = 3). Absorbance data were obtained using a BMG Labtech FLUOstar plate-reader.

Results and discussion

Synthesis and characterisation of nanogels

In this study four nanogels (N-x) systems were prepared (see Scheme 1A). Potentiometric titration data (Fig. S1, ESI† and Table 2) showed the N-1 to N-4 nanogels contained 20.8 to 26.5 mol% MAA and hence high –COOH contents. The apparent pK_a values for N-1, N-2 and N-4 were 7.3, 7.4 and 6.6, respectively. A pK_a range of 6.5–7.0 has been suggested for crosslinked PMAA in the literature.[30] N-3 had the lowest MAA content (20.8 mol%) and the highest pK_a of 8.5, which is due to the lower hydrophilicity for this nanogel. The relatively low pK_a of 6.6 for N-4 is due to the greater mobility of poly(EA) segments. Both of these trends were reported previously for linear poly(EA) and poly(MMA) copolymers containing MAA.[31,32] The present data demonstrate the ability to tune the pK_a within the physiological pH range using nanogel composition. This ability is potentially useful for delivery, diagnostic and biomaterial applications because the pK_a governs the pH where swelling occurs.

The N-x nanogels were first characterised using electron microscopy. Fig. 1a shows a transmission electron microscopy (TEM) image for N-1. Scanning electron microscopy (SEM) images for N-2, N-3 and N-4 are shown in Fig. S2 (ESI†). Based on electron microscope images, the NG particles were not monodisperse. This is because in order to achieve small size particles we used semicontinuous feed method[25] without a seed to prepare the NGs. Whilst this method gave nanogels the consequence was an extended nucleation stage which resulted in increased size polydispersity. The number-average diameters determined from these data (d_{EM}) were 20 to 51 nm (Table 2).

These values are similar to the z-average diameters (d_z) measured at pH 6.0 (Table 2). The latter corresponds to the nanolatex form of the nanogels. The nanogels were pH-responsive

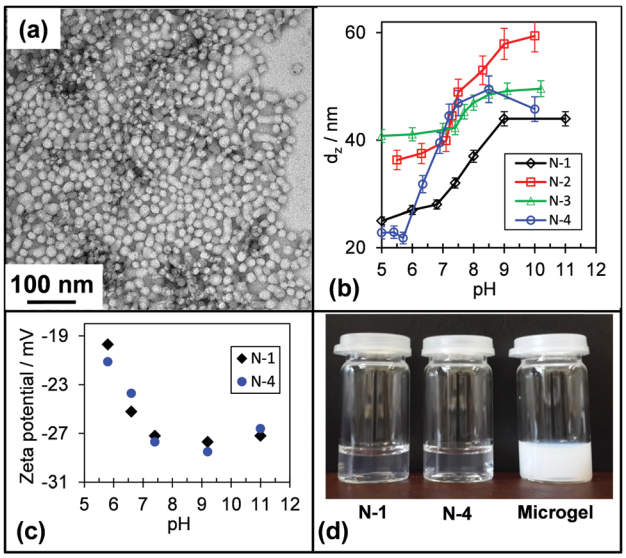

Fig. 1 (a) TEM image for N-1 particles. (b) z-Average diameter (d_z) *vs.* pH. (c) Zeta potential *vs.* pH (the error bars are smaller than the symbols). (d) Sample vials of N-1, N-4 and a microgel dispersion (all 2.0 wt%). The pH values were 5.6, 5.5 and 5.2, respectively.

(Fig. 1b) and the d_z values for N-1, N-2 and N-4 increased strongly as the pH approached the respective apparent pK_a values. N-3, which had the lowest MAA content, showed the smallest pH-triggered d_z increase, as expected. The d_z values for the nanogels at pH 9.0 were 44 to 58 nm and were much less than 100 nm. N-1 to N-4 satisfied the strict size criterion for genuine nanogels.

The surface charge of a particle plays a key role in the interaction with cells[16] and negative charge favours biocompatibility.[33] Zeta potential *vs.* pH curves for N-1 and N-4 (Fig. 1c) showed that the nanogels were negatively charged across the physiological pH range and beyond. The zeta potential is determined by charges near the nanogel surface and its magnitude increased with increasing pH due to –COO^- formation. The dispersions showed excellent optical clarity even when the pH was less than the apparent pK_a and the particles were in their nanolatex form (Fig. 1d). By contrast a control poly(MMA–MAA–EGDMA) microgel dispersion in latex form with a d_z value of 89 nm was turbid (Fig. 1d). The greater turbidity of the microgel dispersion is due to larger size of the particles. It is important to note that light scattering is proportional to the sixth power of particle size.[34] Therefore, larger particles scatter light much more strongly compared to smaller particles.

Table 2 Characterisation data for the nanogels

Code	MAA[a]/ mol%	GMA[b]/ mol%	pK_a[c]	d_{EM}[d]/ nm	$d_{z(coll)}$[e]/ nm	$d_{z(swell)}$[f]/ nm	ζ[g]/mV
N-1	24.0	—	73	20 [4]	27	44	−20
N-2	26.5	—	7.4	41 [8][h]	38	58	−23
N-3	20.8	—	8.5	51 [5][h]	41	49	—
N-4	24.3	—	6.6	28 [4][h]	22	50	−21
N-1G	21.5	2.5	7.1	17 [3]	19	53	−21
N-2G	25.3	4.4	7.3	40 [5][h]	35	105	—
N-3G	18.4	2.4	7.8	—	43	89	
N-4G	20.2	4.1	6.6	32 [3][h]	31	54	−22

[a] Determined from potentiometric titration data shown in Fig. S1 and S3 (ESI). [b] Calculated using the difference of the MAA contents before and after functionalisation. [c] Apparent pK_a value determined from potentiometric titration. [d] Electron microscopy includes SEM and TEM. The number-average diameters are from TEM data unless otherwise stated. The number in the brackets is the standard deviation. [e] Measured at pH values of ~6.0 which corresponds to collapsed particles. [f] Measured at pH ~9.0. [g] Zeta potential measured at pH ~6.0. [h] Number-average diameter determined from SEM data.

Functionalisation of nanogels

Carboxylic acid groups are highly amenable to functionalisation[21] using a range of chemistries. Because of their high MAA contents, our nanogels were well suited to such functionalisation. An epoxide ring-opening[35] reaction between glycidyl methacrylate (GMA) and –COOH at pH 5.1 and 40 °C was used to functionalise the nanogels with vinyl groups (see Scheme 1B and the Experimental section). The GMA contents of the N-xG (x = 1–4) particles were 2.5 to 4.4 mol% as determined from potentiometric titration data

(Fig. S3, ESI† and Table 2). The apparent pK_a values did not change greatly after such GMA functionalisation for N-1G, N-2G and N-4G. The pK_a decreased to 7.8 for N-3G, which is closer to the physiological pH range. TEM (Fig. 2a), SEM images (Fig. S4, ESI†) and d_{EM} values (Table 2) showed that the nanogel morphologies and sizes were not significantly altered by GMA functionalisation.

When compared to the d_z *vs.* pH data for the parent nanogels (Fig. 1b) the GMA-functionalised nanogels N-1G, N-2G and N-3G showed much stronger pH-triggered d_z enhancements than that observed for N-4G (see Fig. 2b). N-1G, N-2G and N-3G were based on glassy poly(MMA); whereas N-4G was based on rubbery poly(EA). The swelling enhancements are interesting. A related effect was reported earlier for microgel particles[2,3] and was attributed to solvent washing. We tentatively attribute the present enhancement to chloroform washing which is proposed to have removed kinetically frozen poly(MMA)-based crosslinks. This effect did not occur for N-4G due to the higher poly(EA) segment mobility. The poly(MMA–MAA–EGDMA) nanogels with a higher crosslink content (N-1) or a lower MAA content (N-3) were designed to keep the d_z values for the functionalised nanogels below 100 nm at high pH.

Because the GMA-functionalised nanogels showed strong pH-triggered particle swelling (Fig. 2b), the rheological properties of concentrated N-1G dispersions were studied. Low viscosity fluids changed to shear-thinning viscous fluids (12 wt%) or free-standing physical gels (21 wt%) at pH 7.4 due to nanogel swelling (Fig. 2c) (dynamic rheology data for the former are shown in Fig. S5, ESI†). At the highest concentration (21 wt%) the frequency-sweep dynamic rheology data (Fig. 2d, top) showed a frequency-dependent storage modulus (G'). This behaviour is expected for soft gels. The strain-sweep data (Fig. 2d, bottom) showed that G' approached the loss modulus (G'') at a strain of 1000%, which indicates that the physical gel was highly ductile. The thixotropic gel was also mouldable. These properties are potentially useful for filling irregularly-shaped voids in tissue repair applications.

From interlinked nanogels to fluorescent hydrogels

The vinyl-functionalised nanogels were covalently interlinked within concentrated dispersions to prepare new elastomeric hydrogels (Scheme 1C). After the dispersions (12 wt%) were mixed with initiator (APS) and accelerator (TEMED), the pH was increased to 7.4 and dispersion transferred to a mould and held at 37 °C. The viscous fluids transformed into hydrogels (Fig. 3a, top left and inset of Fig. 3b) due to free-radical coupling of vinyl groups on neighbouring nanogels. The nanogels acted as macro-crosslinkers and were the only gel building block. The covalent coupling of the peripheral vinyl groups introduced inter-particle crosslinking within DX NGs in addition to the intra-particle crosslinking from EGDMA or BDDA.

The DX NGs were transparent and text was easily visible from behind the gels (Fig. 3a, top left). The UV-visible spectrum for DX N-1G (Fig. 3c) showed that gel disks (1.5 mm thick) had very low absorption values from 350 to 700 nm. DX N-1G gel showed pH-dependent swelling and had a volume–swelling ratio of 17.5 at pH 7.4 (Fig. S6, ESI†). The morphology of freeze dried DX N-1G was examined using SEM (Fig. S7, ESI†). A smooth surface indicated coalescence of NG particles. Clusters of NG particles were also observed within a structural defect.

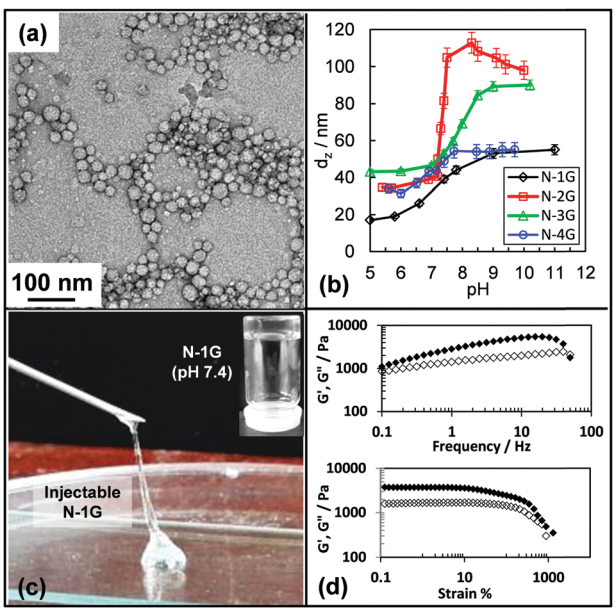

Fig. 2 (a) TEM for N-1G. (b) d_z *vs.* pH. (c) N-1G dispersion injection (12 wt%). The inset is a free-standing physical gel (21 wt%) at pH 7.4. The latter gel was studied by (d) frequency sweep (top) and strain-sweep (bottom) rheology for N-1G. G' (storage modulus) and G'' (loss modulus) are closed and open symbols, respectively.

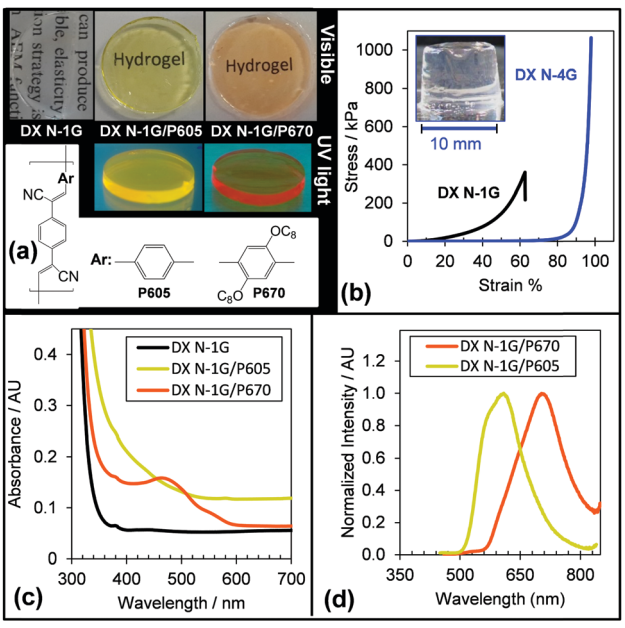

Fig. 3 (a) Images of DX N-1G gel and DX N-1G/PD composites gels using visible (top row) and UV light (second row). The disc diameter for all was 12 mm. (b) Compression stress–strain data and a DX N-4G gel (inset). (c) UV-visible spectra. (d) PL spectra for DX N-1G/P605 (λ_{ex} = 380 nm) and DX N-1G/P670 (λ_{ex} = 450 nm).

MTT assays for nucleus pulposus cells in the presence of DX N-1G showed no detectable cytotoxicity (Fig. S8, ESI†). The use of APS/TEMED initiator system for preparing cell laden acrylate based hydrogels has been reported earlier in the literature.[36] Furthermore, the same initiator system and chemically similar microgel particles were also shown to be biocompatible when nucleus pulposus cells were cultured in the presence of double crosslinked microgels.[26] Thus, it is highly likely that the process here for DX NG formation would not be cytotoxic.

The mechanical properties for DX N-1G and DX N-4G were measured using uniaxial compression (Fig. 3b). The average modulus (E) and strain-at-break (ε_B) values for DX N-1G were 26 kPa and 62%, respectively. By contrast, the E and ε_B values for DX N-4G were 1.0 kPa and $>98\%$. The latter gels were so ductile that the ε_B value could not be measured using our equipment. This remarkable ductility is ascribed to the high mobility of the poly(EA) chains. The contrast in mechanical properties observed (from moderately soft to very soft gels) raises the interesting possibility of E and ductility control *via* selection of the glass transition temperatures of the primary polymer used to construct the parent nanogels. This conjecture will be studied in future work. The DX NGs were also more ductile than comparable MMA- or EA-based DX MGs.[37,38] These differences indicate that lower extents of intra- and/or inter-particle crosslinking were present within the DX NGs.

There has been considerable interest in using conjugated polymer dots (PDs) for *in vivo* imaging due to their bright fluorescence and biocompatibility.[28] We took advantage of the excellent optical clarity of the DX NGs to assemble the first examples of DX NG/PD composite hydrogels. Two PD dispersions were synthesised using colloidal Knoevenagel polymerisation (see Experimental section). P605 and P670 PDs had wavelengths of maximum photoluminescence (PL) emission (λ_{em}) of 605 and 670 nm, respectively (Fig. S9, ESI†). The number-average diameter values for the PDs obtained from TEM data (Fig. S10, ESI†) were 15.2 and 16.2 nm, respectively.

N1-G and P605 or P670 PD dispersions were mixed and cured to give DX N-1G/PD composite gels using the same method used to prepare DX N-1G (Experimental section). These new composite gels contained 3 wt% of PDs based on total solid content. They were coloured under visible light (with text underneath the gels easily visible) and fluorescent when viewed under UV light (Fig. 3a). The UV-visible spectra (Fig. 3c) showed a maximum for DX 1-G/P670. However, the maximum at 325 nm for P605 (Fig. S11, ESI†) was absent for DX N-1G/P605 because of light scattering at wavelengths below 350 nm (Fig. 3c).

PL spectra for the DX N-1G/PD composite gels were also measured (Fig. 3d). The λ_{em} value of 605 nm for DX N-1G/P605 was the same as that for P605 (Fig. S9, ESI†). Interestingly, the PL spectrum for DX N-1G/C670 system had a λ_{em} value of 705 nm, which was red-shifted by $\sim$35 nm compared to the λ_{em} value for P670. This red-shift indicates a change in the electronic state within the original P670 PDs. Such a red-shift is potentially beneficial because it brought the emission further into the near-infrared (NIR) region which is highly penetrating in tissue.[39] These results raise the interesting possibility of using DX N-1G/P670 gels as an injectable imaging gel within the body. This composite hydrogel is also potentially capable of load support. Of course application as an imaging gel would require cytotoxicity investigations for the whole process of DX NG/PD formation, which is beyond the scope of the present study. Considering that the PDs studied here have already been used successfully *in vivo*[28] and the discussion concerning DX NG cytotoxicity presented above there are good grounds to suggest that such an application would be feasible.

Conclusions

We have introduced for the first time a scalable synthesis for pH-responsive polyacid nanogels using a one-step emulsion polymerisation route with swollen diameters below 100 nm. These new particles are a missing link for responsive gel particles. The nanogels remained highly swellable after their functionalisation with GMA and formed injectable fluids that could be transformed into transparent, ductile, elastomeric hydrogels at pH 7.4. DX N-1G was not cytotoxic and formed fluorescent composite gels when assembled with PDs. The DX N-1G/P670 composite gels showed NIR fluorescence and should offer potential for a dual load-supporting/remote imaging system. These new polyacid nanogels are expected to enable synthesis of a wide range of functionalised nanogels, physical gels and covalent gels.

Acknowledgements

BRS and SPA thank the EPSRC for funding (EP/K030949/1 & EP/K03071X/1). We also thank Annie Pallis for assistance.

Notes and references

1 M. Soleimani, J. C. Haley, D. Majonis, G. Guerin, W. Lau and M. A. Winnik, *J. Am. Chem. Soc.*, 2011, **133**, 11299–11307.
2 S. Saxena, C. E. Hansen and L. A. Lyon, *Acc. Chem. Res.*, 2014, **47**, 2426–2434.
3 V. C. Kelessidis, E. Poulakakis and V. Chatzistamou, *Appl. Clay Sci.*, 2011, **54**, 63–69.
4 E. Yilmaz and H.-H. Borchert, *Int. J. Pharm.*, 2006, **307**, 232–238.
5 IUPAC, Compendium of Chemical Terminology, (Gold Book), created by M. Nic, J. Jirat, B. Kosata; updates compiled by A. Jenkins, 2nd edn, ISBN 0-9678550-9-8, doi:10.1351/goldbook.
6 A. C. Brown, S. E. Stabenfeldt, B. Ahn, R. T. Hannan, K. S. Dhada, E. S. Herman, V. Stefanelli, N. Guzzetta, A. Alexeev, W. A. Lam, L. A. Lyon and T. H. Barker, *Nat. Mater.*, 2014, **13**, 1108–1114.
7 T. Rossow, J. A. Heyman, A. J. Ehrlicher, A. Langhoff, D. A. Weitz, R. Haag and S. Seiffert, *J. Am. Chem. Soc.*, 2012, **134**, 4983–4989.
8 T. Ngai, S. H. Behrens and H. Auweter, *Chem. Commun.*, 2005, 331–333.

9 D. Suzuki, S. Tsuji and H. Kawaguchi, *J. Am. Chem. Soc.*, 2007, **129**, 8088–8089.
10 D. Klinger and K. Landfester, *Macromolecules*, 2011, **44**, 9758–9772.
11 I. Gorelikov, L. M. Field and E. Kumacheva, *J. Am. Chem. Soc.*, 2004, **126**, 15938–15939.
12 X. Jia, Y. Yeo, R. J. Clifton, T. Jiao, D. S. Kohane, J. B. Kobler, S. M. Zeitels and R. Langer, *Biomacromolecules*, 2006, **7**, 3336–3344.
13 N. Morimoto, S. Hirano, H. Takahashi, S. Loethen, D. H. Thompson and K. Akiyoshi, *Biomacromolecules*, 2013, **14**, 56–63.
14 G. B. Demirel and R. von Klitzing, *ChemPhysChem*, 2013, **14**, 2833–2840.
15 H. A. Abd El-Rehim, A. E. Swilem, A. Klingner, E.-S. A. Hegazy and A. A. Hamed, *Biomacromolecules*, 2013, **14**, 688–698.
16 H.-Q. Wu and C.-C. Wang, *Langmuir*, 2016, **32**, 6211–6225.
17 W.-H. Chiang, V. T. Ho, W.-C. Huang, Y.-F. Huang, C.-S. Chern and H.-C. Chiu, *Langmuir*, 2012, **28**, 15056–15064.
18 A.-C. Hellgren, P. Weissenborn and K. Holmberg, *Prog. Org. Coat.*, 1999, **35**, 79–87.
19 A. Aymonier, E. Papon, J. J. Villenave, P. Tordjeman, R. Pirri and P. Gérard, *Chem. Mater.*, 2001, **13**, 2562–2566.
20 J.-H. Ryu, R. T. Chacko, S. Jiwpanich, S. Bickerton, R. P. Babu and S. Thayumanavan, *J. Am. Chem. Soc.*, 2010, **132**, 17227–17235.
21 I. Cobo, M. Li, B. S. Sumerlin and S. Perrier, *Nat. Mater.*, 2015, **14**, 143–159.
22 R. Tiwari, T. Heuser, E. Weyandt, B. Wang and A. Walther, *Soft Matter*, 2015, **11**, 8342–8353.
23 R. Liu, A. H. Milani, T. J. Freemont and B. R. Saunders, *Soft Matter*, 2011, **7**, 4696–4704.
24 B. E. Rodriguez, M. S. Wolfe and M. Fryd, *Macromolecules*, 1994, **27**, 6642–6647.
25 J. d. S. Nunes and J. M. Asua, *Langmuir*, 2012, **28**, 7333–7342.
26 A. H. Milani, A. J. Freemont, J. A. Hoyland, D. J. Adlam and B. R. Saunders, *Biomacromolecules*, 2012, **13**, 2793–2801.
27 T. L. Sun, T. Kurokawa, S. Kuroda, A. B. Ihsan, T. Akasaki, K. Sato, M. A. Haque, T. Nakajima and J. P. Gong, *Nat. Mater.*, 2013, **12**, 932–937.
28 S. Kim, C.-K. Lim, J. Na, Y.-D. Lee, K. Kim, K. Choi, J. F. Leary and I. C. Kwon, *Chem. Commun.*, 2010, **46**, 1617–1619.
29 Y. Nomura, R. Horlein, P. Tzallas, B. Dromey, S. Rykovanov, Z. Major, J. Osterhoff, S. Karsch, L. Veisz, M. Zepf, D. Charalambidis, F. Krausz and G. D. Tsakiris, *Nat. Phys.*, 2009, **5**, 124–128.
30 V. Kozlovskaya, E. Kharlampieva, M. L. Mansfield and S. A. Sukhishvili, *Chem. Mater.*, 2006, **18**, 328–336.
31 R. Bird, T. Freemont and B. R. Saunders, *Soft Matter*, 2012, **8**, 1047–1057.
32 O. Pinprayoon, R. Groves and B. R. Saunders, *J. Colloid Interface Sci.*, 2008, **321**, 315–322.
33 Y. Li, D. Maciel, J. Rodrigues, X. Shi and H. Tomás, *Chem. Rev.*, 2015, **115**, 8564–8608.
34 D. H. Everett, *Basic principles of colloid science*, RSC, Cambridge, 1973.
35 A. V. Reis, A. R. Fajardo, I. T. A. Schuquel, M. R. Guilherme, G. J. Vidotti, A. F. Rubira and E. C. Muniz, *J. Org. Chem.*, 2009, **74**, 3750–3757.
36 J. Lam, E. C. Clark, E. L. S. Fong, E. J. Lee, S. Lu, Y. Tabata and A. G. Mikos, *Biomaterials*, 2016, **83**, 332–346.
37 Z. Cui, W. Wang, M. Obeng, M. Chen, S. Wu, I. A. Kinloch and B. R. Saunders, *Soft Matter*, 2016, **12**, 6985–6994.
38 A. H. Milani, J. Bramhill, A. J. Freemont and B. R. Saunders, *Soft Matter*, 2015, **11**, 2586–2595.
39 C. Zhu, L. Liu, Q. Yang, F. Lv and S. Wang, *Chem. Rev.*, 2012, **112**, 4687–4735.